

**Targeting Tryptophan and Tyrosine Metabolism by Liquid Chromatography
Tandem Mass Spectrometry.**

Josep Marcos^{a,b,c}, Nuria Renau^a, Olga Valverde^{a,b}, Gemma Aznar-Lain^d, Irene Gracia-
Rubio^b, Marta Gonzalez-Sepulveda^b, Luis Alberto Pérez-Jurado^{a,b,e}, Rosa Ventura^{a,b},
Jordi Segura^{a,b}, Oscar J. Pozo^{a*}

^a Neuroscience Research Program, Hospital del Mar Research Institute (IMIM), Doctor
Aiguader 88, 08003 Barcelona, Spain

^b Department of Experimental and Health Sciences, Universitat Pompeu Fabra, Doctor
Aiguader 88, 0Toxicology Department,

^c LabcoDiagnostics, Verge de Guadalupe 18, 08950 Esplugues de Llobregat, Spain. 8003
Barcelona, Spain

^d Pediatric Neurology, Hospital del Mar, Barcelona, Spain

^e Centro de Investigación Biomédica en Red de Enfermedades Raras (CIBERER),
Barcelona, Spain

Corresponding author: Óscar J Pozo

Phone: 0034-933160472

Fax: 0034-933160499

E-mail: opozo@imim.es

Abstract

An imbalance in tryptophan (Trp) and tyrosine (Tyr) metabolites is associated with neurological and inflammatory disorders. The accurate and precise measurement of these compounds in biological specimens is a powerful tool to understand the biochemical state in several diseases. In this study, a rapid, accurate and sensitive method based on liquid chromatography-tandem mass spectrometry (LC-MS/MS) for the targeted analysis of the metabolism of Trp and Tyr has been developed and validated. The method allows for the adequate quantification of Trp, Tyr and, eight Trp metabolites, three Tyr metabolites, together with four competitive large neutral aminoacids. Serotonin, 5-hydroxyindoleacetic acid, kynurenine, kynurenic acid, dopamine, and homovanilic acid were among the targeted compounds. Sample preparation, chromatographic separation and mass spectrometric detection were optimized in human urine, human plasma and mice prefrontal cortex extracts. The method was shown to be linear ($r>0.98$) in the range of endogenous concentrations for all studied metabolites. In general, the limits of detection were suitable for the detection of the endogenous levels. Intra- and inter- assay precisions below 25% and accuracies ranging from 80 to 120% were found for most of the analytes. The use of labeled internal standards corrected the moderate matrix effect observed for some compounds. The applicability of the method was confirmed by analyzing urine samples collected from 13 healthy volunteers and comparing the results with previously established normal ranges. In addition, urine samples from two patients and a heterozygous carrier of a family with disturbed monoamine metabolism due to a loss of function mutation in the *MAOA* gene (X-linked) were analyzed and compared with samples from controls. All data together show the potential of the developed approach for targeted metabolomic studies.

Keywords: Tryptophan, tyrosine, kynurenine, metabolites, mass spectrometry,
quantitative method

Highlights

- An LC-MS/MS method for the study of tryptophan and tyrosine metabolism is presented
- Concurrent quantification of 4 competitive large neutral aminoacids is offered
- Fully validated in human serum and urine, and in mice prefrontal cortex extracts
- Urinary concentrations for 18 analytes in 13 healthy individuals were calculated
- Applicability proved by analyzing samples from a family with the Brunner syndrome

1. Introduction

The aromatic and essential amino acids phenylalanine (Phe), tyrosine (Tyr) and tryptophan (Trp) are converted to catecholamines and serotonin (5-HT) by enzymes in adrenal, intestinal and nervous tissue [1]. Imbalances on these pathways are associated with several neurological and inflammatory disorders.

Trp is an essential amino acid necessary for protein biosynthesis and also the precursor of a large number of biologically active metabolites [2]. Trp is metabolized via several pathways, the major ones being the 5-HT and kynurenine (Kyn) pathways (Figure 1). Trp depletion or the imbalance in its metabolic products can have pathophysiological implications [3-5].

5-HT, is an important neurotransmitter that modulates numerous behavioral and physiological functions such as sleep, mood, appetite, learning, and memory [6]. Recent studies have demonstrated decreased levels of cortical 5-HT in neonatal animals with cerebral palsy induced by maternal-fetal inflammation [7]. An elevated urinary concentration of its metabolite, 5-hydroxyindoleacetic acid (5-HIAA), is used as a biochemical test for the diagnosis of a carcinoid tumor [8], as well as for the diagnosis of phenylketonuria, and migraine [9].

The kynurenine pathway is composed of two branches, leading to either the formation of kynurenic acid (KA) and xanthurenic acid (XA) or to the generation of 3-hydroxyanthranilic acid (3OH-AA) and quinolinic acid [10]. Whereas KA, an N-methyl-D-aspartate receptor antagonist, is considered to be neuroprotective [11], the metabolic products of the other branch, including 3OH-AA and quinolinic acid, are considered to be neurotoxic [12]. Imbalances in the kynurenine pathway have been related with several pathological conditions like schizophrenia [13], major depression [14], autism and epilepsy [15], or Alzheimer disease [16].

On the other hand, Tyr is synthesized from the essential amino acid Phe by the action of the enzyme phenylalanine hydroxylase. Plasma Tyr has been proposed as a useful assessment of thyroid function [17]. The main metabolic pathway for Tyr involves its transformation in the neurotransmitter dopamine (DA). DA is subsequently metabolized into several metabolites like 3-methoxytyramine (3Me-Ty) and homovanillic acid (HVA) (Figure 1). Quantification of the major urinary product HVA and others catecholamine metabolites is routinely performed in patients suspected of having neuroblastoma or pheochromocytoma [18].

The rate of brain 5-HT and DA synthesis depends on the Trp and Tyr concentration respectively [19,20], which in turn depends on the ratio between plasma concentration of Trp/Tyr and other large neutral amino acids (LNAAs) that compete for blood-brain barrier (BBB) transport [21]. These LNAAs are Phe, leucine (Leu), isoleucine (Ile), valine (Val) and methionine (Met) [19,22]. It has been proved that, depending on the dietary intake of these amino acids, there can be substantial differences in the plasmatic ratios Trp/LNAAs and Tyr/LNAAs, with subsequent consequences on the catecholamine synthesis in the brain [23].

In summary, the accurate and precise measurement of these compounds in biological specimens is a powerful tool to understand the biochemical state in several diseases. To date, a number of methods for the analysis of Trp and its metabolites have been developed, mostly based on liquid or gas chromatography with various detection modalities, such as UV absorbance, fluorescent, and electrochemical [24-28]. However, if multiple species need to be analyzed with high sensitivity, which is very useful when a small amount of sample is available, then the use of mass spectrometers is preferred [29]. Thus, several LC-MS/MS methods have been recently developed for the detection of Trp and some of its metabolites [30-32], as well as for Tyr and its metabolites [33].

The use of LC-MS/MS instruments allows for the simultaneous quantification of targeted components of different metabolic routes, thus providing a more comprehensive picture of the biological changes in a single analysis. Moreover, these targeted strategies can easily incorporate some other analytes of interest that are not directly involved in the Trp and Tyr metabolic routes, such as the rest of LNAAs. To our knowledge, there is not any published method for the simultaneous determination of the complete panel of Trp and Tyr metabolites and LNAA competitors.

The first goal of the present study was to develop and validate a suitable method for the simultaneous quantification of Trp, Tyr, their metabolites, and their LNAA competitors in three different biological matrices; human urine, human plasma and murine prefrontal cortex (PFC) homogenates. The second aim was to demonstrate the clinical application of this targeted metabolomic approach in urine samples. For this purpose, a cohort of healthy individuals (n=13) was analyzed and the values obtained with the present method compared with the previously reported. Additionally, spot urine samples from three individuals from a family with the Brunner syndrome, a rare X-linked genetic disorder caused by a mutation in the Monoamineoxidase A (*MAOA*) gene that leads to an excess of monoamines in the brain [34,35], were analyzed and the results compared with spot urine samples collected from a control group.

2. Material and methods

2.1. Chemicals and reagents

Phenylalanine (Phe), valine (Val), leucine (Leu), isoleucine (Ile), methionine (Met), tryptophan (Trp), serotonin (5-HT), 5-hydroxyindoleacetic acid (5-HIAA), kynurenine (Kyn), 3-hydroxykynurenine (3OH-Kyn), anthranilic acid (AA), 3-hydroxyanthranilic acid (3OH-AA), kynurenic acid (KA), xanthurenic acid (XA), tyrosine (Tyr), dopamine (DA), 3-methoxytyramine (3Me-Ty), homovalinic acid (HVA), ammonium formate (HPLC grade), EDTA and other reagents for tissue purification were purchased from Sigma-Aldrich (St Louis, MO, USA). Dopamine-d₄ (DA-d₄), kynurenic acid-d₅ (KA-d₅), phenylalanine-d₅ (Phe-d₅) and serotonin-d₅ (5HT-d₅) were supplied by Toronto Research Chemicals (Toronto, Canada). Tyrosine-d₄ (Tyr-d₄), tryptophan-d₅ (Trp-d₅), 3-methoxytyramine-d₄ (3Me-Ty-d₄), 5-HIAA-d₄, 3OH-Kyn-¹³C₆, and Kyn-¹³C₆ were from Alsachim (Illkirch-Graffenstaden, France). Formic acid (LC/MS grade), acetonitrile and methanol (LC gradient grade) were obtained from Merck (Darmstadt, Germany). Ultrapure water was obtained using a Milli-Q purification system (Millipore Ibérica, Barcelona, Spain). For structures of the analytes see Figure 1.

2.2. Instrumentation

We used an Acquity UPLC system, (Waters Associates) for the chromatographic separation coupled to a triple quadrupole (Quattro Premier XE) mass spectrometer provided with an orthogonal Z-spray-electrospray interface (ESI) (Waters Associates, Milford, MA, USA). The drying and nebulising gas was nitrogen. The desolvation gas flow was set to approximately 1200 L h⁻¹ and the cone gas flow to 50 L h⁻¹. A capillary voltage of 3 kV was used in positive ionization mode. The nitrogen desolvation

temperature was set to 450°C and the source temperature to 120°C. Collision gas was argon at a flow of 0.21 ml/min. The injection volume was 10 µl.

The LC separation was performed at 55 °C using an Acquity BEH C₁₈ column (100 mm, 2.1 mm i.d., 1.7 µm) (Waters Associates), at a flow rate of 300 µL min⁻¹. Water and methanol both with formic acid (0.01% v/v) and ammonium formate (1mM) were selected as mobile phase solvents. A gradient program was used for the separation of the analytes; the percentage of (B) solvent was linearly changed as follows: 0 min, 1%; 0.5 min, 1%; 7 min, 40%; 8.5 min, 90%; 9 min, 90%; 9.5 min, 1%; 12 min, 1%. The analysis was performed in a total run time of 12 min.

Analytes were determined by a Selected Reaction Monitoring (SRM) method by acquiring two transitions for each compound (**Table 1**). The most specific transition was selected for quantitative purposes. MassLynx software was used for data management.

2.3. Biological samples

2.3.1. Murine prefrontal cortex homogenates

Four male and five female CD1 outbred mice purchased from Charles River (Barcelona, Spain) and shipped to our animal facility (Ubiomex, PRBB) were used for this study. Animals were 10-15 weeks old at the start of the study. Mice were housed in standard cages in a temperature (21°± 1°C), humidity (55% ± 10%), and light-cycle controlled room. Food and water were available *ad libitum*. Male and female mice were allowed to acclimatize to the new environmental conditions for at least one week before starting the experiments. To obtain the brain samples, mice were sacrificed by decapitation and brains were rapidly removed. Prefrontal cortex area (PFC) was dissected using a brain tissue blocker. All samples were immediately frozen in dry ice and stored at -80°C. Every effort

was made to minimize the number of animals. . All procedures were conducted in accordance with the guidelines of the European Community, Directive 2010-63EU and BOE-2013-1337 regulating animal research and approved by the local ethical committee (CEEA-PRBB).

2.3.2. Human urine sample collection

Spot urine samples collected from six healthy volunteers were used for the validation of the method. In order to evaluate the applicability of the developed method, 24h urine samples (complete amount of urine excreted in one day) collected from 13 healthy Caucasian volunteers (8 males, 26-41 years-old and 5 females, 23-67 years-old) were analysed. Results were compared with normal ranges previously reported.

Spot urine samples from three recently described individuals (two affected brothers and the carrier mother) with documented loss of function mutations in the X-linked *MAOA* gene were obtained [36]. The older brother had a diagnosis of pervasive developmental disorder not otherwise specified while the younger fulfilled criteria for autism with moderate intellectual disability and abnormal and impulsive behavior. The mother (mutation carrier) presented with a depressive disorder and there was a history of psychiatric disease in other unavailable maternal relatives, consistent with X-linked pattern of inheritance. Results were compared with spot urines collected from 30 healthy volunteers. Additional clinical studies (performed at the clinical laboratories, Hospital del Mar) included levels of normetanephrine, serotonin and related metabolites (vanilmandelic acid, HVA and 5-HIAA) in blood and 24h urine samples. Both brothers had a documented disturbance of the catecholamine and serotonin metabolism with high

levels of 5-HT (2x), and normetanephrine (2,4x) as well as other catecholamine metabolites in blood and urine, milder in their mother.

Urinary concentrations of creatinine were determined by standard methods using ADVIA 2400 equipment (Siemens Medical Solutions Diagnostics, Tarrytown, NY, USA).

2.3.3 Human plasma collection

Human plasma samples used for method validation were obtained by arm venipuncture from six healthy volunteers at the hospital facilities. Plasma samples were collected in tubes containing EDTA as anticoagulant.

2.4. Sample preparation

2.4.1. Internal standard mixture

An internal standard mixture containing 1000 ng/mL of 5HIAA-d₄, 500 ng/mL of Tyr-d₄, 500 ng/mL of 3OH-Kyn-¹³C₆, 500ng/mL of Trp-d₅, 500 ng/mL of Phe-d₅, 500 ng/mL of 5HT-d₅, 100 ng/mL of Kyn-¹³C₆, 100 ng/mL of DA-d₄, 50 ng/mL of 3Me-Ty-d₄ and 50 ng/mL of KA-d₅ was prepared by dissolving the appropriate amounts of the stock solutions in a mixture methanol:ascorbic acid 20mM (1:1; v:v). The same internal standard mixture was used for all determinations.

2.4.2. Urine

An aliquot of 100 µL of urine was 10 fold diluted with water. After mixing, 75 µL of the internal standard mixture were added together with 75 µL of the diluted extract into the injection vial, and 10 µL were injected into the system.

228

229 2.4.3. Plasma

230 An aliquot of 150 μ L of plasma was mixed with 300 μ L of acetonitrile in order to
231 precipitate the proteins. After centrifugation, the supernatant was transferred to a clean
232 tube and 50 μ L of the internal standard mixture were added. The mixture was evaporated
233 at room temperature under nitrogen stream (<10 psi). After reconstitution with 150 μ L of
234 water, 10 μ L were injected into the system. The standards used for calibration were
235 subjected to the sample procedure.

236

237 2.4.4. PFC homogenates

238 For the tissue processing, after adding 500 μ l of ice-cold buffer (0.5 mN sodium
239 metabisulfate, 0.2 N perchloric acid and 0.5 mM EDTA), the tissue ($15,36 \pm 0,68$ mg)
240 was homogenized using a sonicator [37]. Then, samples were centrifuged 10 min (10.000
241 g at 4°C) and the supernatant was kept on ice until analysis.

242 Two alternative treatments were tested in the analysis of PFC homogenates. On one hand,
243 75 μ L of the PFC extract was mixed with 75 μ L of the internal standard mixture and 10
244 μ L of the diluted extract were injected into the system. On the other hand, 75 μ L of the
245 internal standard mixture was added into 400 μ L of the PFC extract. The mixture was
246 evaporated at room temperature under nitrogen stream (<10 psi). After reconstitution with
247 75 μ L of water, 10 μ L were injected into the system. All the analytes were detected by
248 the first method except for KYN, 3OH-KYN, AA and 3Me-Ty for which the
249 preconcentration step was necessary. The standards used for calibration were subjected
250 to the sample procedure.

251

2.5. Method validation

2.5.1. Linearity

The samples selected for validation were analyzed using the described sample treatment and their concentration estimated against a calibration curve made in water. Calibration standards at seven concentration levels were prepared in ultrapure water for each analyte. The calibration range depended on the basal concentrations expected for the analytes in the matrices tested. Calibration standards were analyzed and calibration curves were calculated by least-squares linear regression. The method was considered linear in the selected range if a correlation coefficient (r) higher than 0.98 was obtained.

2.5.2. Intra-assay accuracy and precision

Precision and accuracy of the method were checked by analyzing quality control samples (QCs). QCs ($n=6$) were prepared by spiking real samples at the second-to-lowest concentration level of the calibration curve. Six different samples were used for this purpose. Since selected analytes are endogenous compounds ubiquitously present in the selected matrices, QCs were always analyzed together with their unspiked extract. The spike concentration was calculated by subtracting the concentration obtained for the unspiked sample to the one of the QC.

Intra-assay precision of the method is expressed as the relative standard deviation (%) of the estimated concentrations obtained for the six QCs analyzed in one assay. Intra-assay accuracy is expressed as the recovery value (%) estimated for the QCs.

2.5.3. Inter-assay accuracy and precision

Inter-assay precision is given as the relative standard deviation (%) of the estimated concentrations obtained for all replicates analyzed along the three validation assays and by two different operators (n=12). Inter-assay accuracy is obtained as described for intra-assay accuracy but considering the replicates analyzed in the three analytical batches (n=12).

2.5.4 Limit of detection (LOD)

The LOD, defined as the lowest concentrations with a value of the signal/noise ratio (S/N) of 3, was calculated by estimating the S/N from the chromatogram at the lowest concentration assayed. Establishing LODs for compounds that are endogenously present at large concentrations is of little interest. Therefore, for those compounds showing a S/N higher than 50 at the lowest calibration level, their LODs were fixed at 1/10 of the lowest calibration level.

2.5.5 Matrix effect

Due to the impossibility to obtain real blank samples, the estimation of the matrix effect was calculated by comparison between the response of the analyte in the QC (after subtraction of the response for the blank sample) and the one of a solvent standard at the same concentration. No correction of the internal standard was made for the calculation of the matrix effect.

3. Results and discussion

3.1. Method optimization

3.1.1. Sample preparation optimization

Sample procedure was optimized in order to detect the endogenous levels of the analytes performing the minimum number of treatment steps. Dilute-and-shoot based approaches are the option of choice for this purpose [38]. Thus, the use of derivatization agents, employed in other validated methods for enhancing the sensitivity, was discarded [32].

In the case of urine, a twenty fold dilution of the sample was adequate for the appropriate quantification of all analytes. This dilution also improved the chromatographic behavior of very polar compounds such as DA, which was found to be substantially altered by the presence of urinary components (Figure 2a and 2b).

Sample treatment for plasma samples involved a simple protein precipitation step, evaporation and reconstitution. The evaporation step was needed in order to eliminate the excess of acetonitrile that will disturb the chromatographic behavior of the most polar metabolites. The evaporation step was performed at room temperature under low nitrogen pressure (< 10 psi) in order to minimize the losses by evaporation. In any case, the addition of isotope-labeled internal standards corrected for any eventual evaporation of the analytes. The method for plasma samples did not involve any dilution or concentration factor. Under these conditions, analytes from all selected pathways were detected except for DA and their metabolites that are present in plasma at trace levels [39]. Some metabolites of the kynurenine pathway (XA and 3OH-AA) remained also undetectable.

In the case of PFC homogenates, a two-fold dilution of the sample allowed for the detection of the aminoacids, 5-HT, 5-HIAA and DA. In order to have information about the kynurenine pathway, a preconcentration step (five fold concentration factor) was

necessary. This concentration factor was achieved by evaporation at room temperature under nitrogen stream (<10 psi).

3.1.2. Liquid chromatographic and mass spectrometric optimization

The high polarity of the selected analytes hampers their retention in C18 columns. In the interest of maximizing this retention, methanol was preferred as organic solvent. In order to obtain suitable retention a 10 cm column was used and the chromatographic gradient started with a high percentage of aqueous solvent (99%). As explained below, the addition of ammonium in the mobile phase was found to be necessary for the proper ionization of HVA.

Most of the analytes are nitrogen-containing molecules and therefore are easily ionizable as $[M+H]^+$ (Table 1). Most of the quantitative transitions have the protonated ion as the precursor ion. The only exception was HVA. The absence of a nitrogen atom in this molecule hampered its detection in positive ionization mode. In fact, it could not be detected when formic acid was used as the only modifier in the mobile phase. However, the addition of ammonium in the mobile phase made possible the formation of the $[M+NH_4]^+$. The most specific and sensitive transitions for HVA were obtained by selecting the $[M+NH_4-NH_3]^+$ as precursor ion.

Two transitions were optimized for each analyte (Table 1). The most sensitive and specific one was used for quantification, the second one for qualitative purposes. All the potential precursor ions of each analyte were fragmented at several collision energies (from 5 eV to 50 eV) and the resulting transitions were tested in terms of specificity and sensitivity. In general, the most abundant transitions were specific enough for the detection of the analytes at the endogenous levels. The main exception was found in the

detection of Leu and Ile. Both analytes shared the transition $132 \rightarrow 86$ (coming from the neutral loss of HCOOH), this fact together with their similar retention times made the quantification of both analytes difficult (Figure 2c). The selection of specific transitions ($132 \rightarrow 43$ for Leu and $132 \rightarrow 69$ for Ile) helped in the proper quantification of both analytes (Figure 2d). Regarding the second transition, in most of the cases the precursor ion for this second transition was the same selected for the first one. However, for some analytes such as 5-HT, 3OH-AA, DA and 3Me-Ty more sensitive results were obtained when $[\text{M}+\text{H}-\text{NH}_3]^+$ or $[\text{M}+\text{H}-\text{H}_2\text{O}]^+$ were selected as precursor ions (Table 1).

3.2. Method validation

Due to the fact that electrospray ionisation is particularly prone to matrix effects, and that this effect may notably vary between different types of specimens, the present method has been independently validated in three different biological matrices; human urine, human plasma and homogenates from mouse brain. The use of adequate internal standards is one of the most suitable approaches to compensate this matrix effects. For this reason, the concentration of each analyte was calculated by using the internal standard closely eluted (Table 2).

Since all the analytes are endogenous, they are present in all matrices studied, making impossible obtaining an analyte-free matrix for conducting the validation experiments. The use of artificial matrices for the validation was considered as alternative but the idea was rejected, as these artificial matrices do not contain most of the interferences present in the real ones. For this reason, the calibrators were prepared in ultrapure water, and precision and accuracy were evaluated in real samples by comparison between the concentrations before and after the addition of known amount of the analytes.

The linearity range to be tested was established for each analyte depending on their expected concentration in each matrix. For this purpose, five samples of each matrix were analyzed by the optimized method and the concentration for each analyte was estimated. Linearity range and QC concentrations for the accuracy and precision experiments were selected on the basis of these ranges (see experimental section). The linear range obtained for each analyte is depicted in Table 2. Satisfactory correlation coefficients ($r > 0.99$) were obtained for all analytes in the selected range (Table 2). The only exception was 3OH-Kyn in both human urine and plasma where correlation coefficients of $r = 0.983$ and $r = 0.982$, respectively were calculated.

The LOD is not an issue for the determination of compounds present in high amounts. In those cases where the S/N at the lowest calibration level was higher than 50, the LOD was arbitrarily fixed at 1/10 of the lowest calibration level assayed. That was the case of aminoacids and Kyn in plasma and Trp, Tyr, Phe, 5-HIAA and KA in urine. For the rest of analytes, the LODs in the three matrices assayed are summarized in Table 2. They range from 0.1 ng mL^{-1} for Kyn, KA and 3Me-Ty in mice PFC homogenates to $1 \text{ } \mu\text{g/mL}$ for HVA in urine.

Low to moderate matrix effects produced by the components of the different matrices were found. The observed concentration due to either ion suppression or ion enhancement ranged typically from 51% to 131% of the spiked value (Table 3). The most suppressed compounds (50-60% for Val, DA and 5HT) showed short retention times being the co-eluting interferences at these retention times the main potential reason for the suppression. Three main exceptions were found in mice PFC homogenates, where Kyn, 3OH-Kyn and KA showed higher ion enhancements, causing an over quantification. Thus, for these three analytes the use of labelled ISTDs, like the ones employed in the present method, is mandatory in order to overcome this problem.

The influence of the different samples on matrix effect in the three selected matrices was evaluated by means of the RSD of the effect observed in six different samples for each type of matrix. RSDs lower than 25% were typically obtained indicating low variation between samples. Met and 5-HT in mice PFC were the only exceptions showing RSD of 30% and 35%, respectively. Once again, the use of labelled ISTDs allowed for the correction of this variation. The low sample volume used for the determination is probably the main reason of the low variation observed, despite the large variability of the matrix components.

Intra-day accuracies ranged from 86 to 117% for all validated compound in the three types of biological specimens. Inter-day accuracies were between 80 and 120%. That confirmed the satisfactory quantitative figures of the developed method.

Regarding precision, the validation results indicate that for the majority of the quantifications the RSDs were below 15%, the only exceptions being Met in PFC, and 3OH-Kyn in urine that showed RSD of 22% and 18% respectively. As expected, the estimation of the inter-day precisions gave RSD values a bit higher, but below the 25% mark for all cases with the only exception of Met in PFC samples which showed a RSD of 35%.

3.3 Method application

3.3.1. Urine samples from healthy individuals

The applicability of the method was tested by the analysis of 24 h urine samples collected from 13 healthy volunteers (8 males and 5 females). Typical chromatograms for a male urine sample are shown in Figure 3. The validated method was able to determine the 18 targeted metabolites and LNAAs in all urine samples (Table 4).

To overcome the possible different diuresis among individuals, clinical urinary determinations are typically normalized either by the urinary concentration of creatinine or by the total volume of urine excreted in a 24 hours period. In order to make our results comparable to the ranges presented by other studies, the results found in this work are presented in both formats (Table 4).

In general, and despite the large variability of published concentrations, results were in agreement with the reported reference values confirming the suitability of the method for the quantification of Trp, Tyr, their metabolites and other LNAAs in human urine samples. It is important to emphasize that these concentrations have been found in healthy adults not taking any type of medications. The urinary concentrations of some Kyn and Tyr metabolites are increased during pregnancy and by contraceptive and corticosteroid hormones [40,41].

3.3.2. Urine samples from MAO-A deficient individuals

The majority of 5-HT is metabolized to 5-HIAA being the flavoprotein MAO (EC 1.4.3.4) the responsible of this transformation. This enzyme is mainly located in mitochondria and catalyses oxidative deamination of several monoamines to their corresponding aldehydes, ammonia and hydrogen peroxide. Two forms of MAO, are known; MAO-A and MAO-B, MAO-A having the highest affinity for 5-HT [42].

Individuals carrying a loss of function mutation in the *MAOA* gene and deficient MAO-A activity do not appropriately metabolize 5-HT, thus leading to abnormal urinary concentration of 5-HT. This build up in the 5-HT production can be easily detected by monitoring two different metabolic precursor/product ratios. As illustrated in Figure 4, in one hand the accumulation of 5-HT leads to an abnormally high ratio when compared to its precursor (Trp). On the other hand, the inability to convert 5-HT to 5-HIAA causes an

442 abnormal 5-HT/5-HIAA ratio. There was a good correlation of the metabolic abnormality
443 with the genotype and also with the neurobehavioral phenotype, with more severe
444 disturbance in the hemizygous males and milder alteration in the heterozygous female
445 (the mother).

4. Conclusions

An LC-MS/MS method for the simultaneous quantitation of Tyr, Trp, their metabolites and competitive LNAA has been developed and validated. The present method has been independently validated in three different biological matrices; human urine, human plasma and homogenates from murine PFC. These are the specimens commonly available when conducting investigations related to the Trp and Tyr metabolism.

The adequacy of the method for its intended purpose in terms of sensitivity, precision, accuracy and linearity has been proven through the application of a validation protocol.

Regarding human samples, the ranges for a set of healthy individuals have been determined by the new method. The figures obtained for those 18 target compounds are in agreement with previously published data.

The wide coverage of Trp and Tyr metabolism, together with short analysis time, low sample volume, simple sample preparation and satisfactory quantitative results make this method useful for targeted metabolomic studies. From a clinical point of view, a change in the relative ratios of these metabolites can provide important insights in predicting the presence and progression of neuroinflammation in disorders such as cerebral palsy, autism, multiple sclerosis, Alzheimer disease, major depression and schizophrenia.

In addition of being a clinical tool for humans, the adequate results obtained for mice PFC homogenates indicates that the validated methodology can also be used in targeted metabolomic studies with animal models dealing with the biosynthesis and metabolism of Trp and Tyr in the brain [43].

Acknowledgements

471 This work was supported by grants from Instituto de Salud Carlos III FEDER,
472 (PI14/00147, RD12/028/024 and PI13/) and MINECO (SAF2013-41761-R). Support of
473 the Generalitat de Catalunya (2009SGR00492, 2014SGR34 and 2014SGR1468 to the
474 research teams) is also acknowledged.
475 Spanish Health National System is acknowledged for O. J. Pozo contract (MS10/00576).

476

477

References

- [1] The Significance of Tryptophan, Phenylalanine, Tyrosine, and Their Metabolites in the Nervous System. S.N. Young. HANDBOOK OF NEUROCHEMISTRY, Vol. 3 (2nd Ed.) Edited by Abel Lajtha (Plenum Publishing Corporation, 1983).
- [2] de Jong WH, Smit R, Bakker SJ, de Vries EG, Kema IP. Plasma tryptophan, kynurenine and 3-hydroxykynurenine measurement using automated on-line solid-phase extraction HPLC-tandem mass spectrometry. *J Chromatogr B Analyt Technol Biomed Life Sci.* 2009;877(7):603-609.
- [3] Reilly JG, McTavish SF, Young AH. Rapid depletion of plasma tryptophan: a review of studies and experimental methodology. *J Psychopharmacol.* 1997;11(4):381-392.
- [4] Toker L, Amar S, Bersudsky Y, Benjamin J, Klein E. The biology of tryptophan depletion and mood disorders. *Isr J Psychiatry Relat Sci.* 2010;47(1):46-55.
- [5] Kegel ME, Bhat M, Skogh E, Samuelsson M, Lundberg K, Dahl ML, Sellgren C, Schwieler L, Engberg G, Schuppe-Koistinen I, Erhardt S. Imbalanced kynurenine pathway in schizophrenia. *Int J Tryptophan Res.* 2014; 7:15-22.
- [6] Schloss P, Williams DC. The serotonin transporter: a primary target for antidepressant drugs. *J. Psychopharmacol.* 1998; 12:115–121.
- [7] Kannan S, Saadani-Makki F, Balakrishnan B, Dai H, Chakraborty PK, Janisse J, Muzik O, Romero R, Chugani DC. Decreased cortical serotonin in neonatal rabbits exposed to endotoxin in utero. *J. Cereb. Blood Flow Metab.* 2011; 31:738–749.
- [8] Rorstad O. Prognostic indicators for carcinoid neuroendocrine tumors of the gastrointestinal tract. *J. Surg. Oncol.* 2005; 89:151–160.
- [9] Bousser MG, Elghozi JL, Laude D, Soisson T. Urinary 5-HIAA in migraine: evidence of lowered excretion in young adult females. *Cephalalgia.* 1986 6(4):205-209.
- [10] Stone TW, Forrest CM, Darlington LG. Kynurenine pathway inhibition as a therapeutic strategy for neuroprotection. *FEBS J.* 2012;279(8):1386-1397.
- [11] Klein C, Patte-Mensah C, Taleb O, Bourguignon JJ, Schmitt M, Bihel F, Maitre M, Mensah-Nyagan AG. The neuroprotector kynurenic acid increases neuronal cell survival through neprilysin induction. *Neuropharmacology.* 2013;70:254-260.

507 [12] Schwarcz R, Whetsell WO, Mangano RM. Quinolinic acid – an endogenous
508 metabolite that produces axon-sparing lesions in rat-brain. *Science*. 1983; 219: 316–318.

509 [13] Schwarcz R, Rassoulpour A, Wu HQ, Medoff D, Tamminga CA, Roberts RC.
510 Increased cortical kynurenate content in schizophrenia. *Biol. Psychiatry*. 2001; 50:521-
511 530.

512 [14] Müller N. Immunology of major depression. *Neuroimmunomodulation* 2014;21(2-
513 3):123-130.

514 [15] Schwartz CE. Aberrant tryptophan metabolism: the unifying biochemical basis for
515 autism spectrum disorders? *Biomark Med*. 2014;8(3):313-315.

516 [16] Chugani DC. Serotonin in autism and pediatric epilepsies. *Ment Retard Dev Disabil*
517 *Res Rev*. 2004; 10(2):112-116. [15] Baran H, Jellinger K, Derecke L. Kynurenine
518 metabolism in Alzheimer’s disease. *J. Neural Transm*. 1999; 106:165–181.

519 [17] Siersbaek-Nielsen K. Determination of the Plasma Tyrosine in Thyroid Disorders.
520 A New Test of Thyroid Function. *Acta Med Scand* 1966; 179(4): 417-426.

521 [18] Rosano TG, Swift TA, Hayes LW. Advances in catecholamine and metabolite
522 measurements for diagnosis of pheochromocytoma. *Clin Chem* 1991;37:1854-1867.

523 [19] Fernstrom JD, Wurtman RJ. Brain serotonin content: physiological regulation by
524 plasma neutral amino acids. *Science*. 1972;178(4059):414-416.

525 [20] Wurtman RJ, Hefti F, Melamed E. Precursor control of neurotransmitter synthesis.
526 *Pharmacol Rev*. 1980;32(4):315-335.

527 [21] Pardridge WM, Oldendorf WH. Kinetic analysis of blood-brain barrier transport of
528 amino acids. *Biochim Biophys Acta*. 1975;401(1):128-136.

529 [22] Fernstrom JD, Faller DV. Neutral amino acids in the brain: changes in response to
530 food ingestion. *J Neurochem*. 1978;30(6):1531-1538.

531 [23] Wurtman RJ, Wurtman JJ, Regan MM, McDermott JM, Tsay RH, Breu JJ. Effects
532 of normal meals rich in carbohydrates or proteins on plasma tryptophan and tyrosine
533 ratios. *Am J Clin Nutr*. 2003;77(1):128-132.

534 [24] Shibata K. Fluorimetric micro-determination of kynurenic acid, an endogenous
535 blocker of neurotoxicity, by high-performance liquid chromatography. *J. Chromatogr*.
536 1988; 430:376–380.

537 [25] Herve C, Beyne P, Jamault H, Delacoux E. Determination of tryptophan and its
538 kynurenine pathway metabolites in human serum by high-performance liquid
539 chromatography with simultaneous ultraviolet and fluorimetric detection. *J. Chromatogr.*
540 *B.* 1996; 675:157–161.

541 [26] Widner B, Werner ER, Schennach H, Wachter H, Fuchs D. Simultaneous
542 measurement of serum tryptophan and kynurenine by HPLC. *Clin. Chem.* 1997; 43:2424–
543 2426.

544 [27] Zagajewski J, Drozdowicz D, Brzozowska I, Hubalewska-Mazgaj M, Stelmaszynska
545 T, Laidler PM, Brzozowski T. Conversion L-tryptophan to melatonin in the
546 gastrointestinal tract: the new high performance liquid chromatography method enabling
547 simultaneous determination of six metabolites of L-tryptophan by native fluorescence and
548 UV-VIS detection. *J. Physiol. Pharmacol.* 2012; 63:613–621.

549 [28] Lesniak WG, Jyoti A, Mishra MK, Louissaint N, Romero R, Chugani DC, Kannan
550 S, Kannan RM. Concurrent quantification of tryptophan and its major metabolites. *Anal*
551 *Biochem.* 2013;443(2):222-231.

552 [29] Segura J, Artigas F, Martinez E, Gelpi E. Adsorption of tryptophan metabolites from
553 physiological fluids on XAD-2 and determination by single ion monitoring. *Biomed Mass*
554 *Spectrom.* 1976;3(2):91-96.

555 [30] González RR, Fernández RF, Vidal JL, Frenich AG, Pérez ML. Development and
556 validation of an ultra-high performance liquid chromatography-tandem mass-
557 spectrometry (UHPLC-MS/MS) method for the simultaneous determination of
558 neurotransmitters in rat brain samples. *J Neurosci Methods.* 2011;198(2):187-194.

559 [31] He B, Bi K, Jia Y, Wang J, Lv C, Liu R, Zhao L, Xu H, Chen X, Li Q. Rapid analysis
560 of neurotransmitters in rat brain using ultra-fast liquid chromatography and tandem mass
561 spectrometry: application to a comparative study in normal and insomnic rats. *J Mass*
562 *Spectrom.* 2013;48(8):969-978.

563 [32] Zheng X, Kang A, Dai C, Liang Y, Xie T, Xie L, Peng Y, Wang G, Hao H.
564 Quantitative analysis of neurochemical panel in rat brain and plasma by liquid
565 chromatography-tandem mass spectrometry. *Anal Chem.* 2012;84(22):10044-10051.

566 [33] Lionetto L, Lostia AM, Stigliano A, Cardelli P, Simmaco M. HPLC-mass
567 spectrometry method for quantitative detection of neuroendocrine tumor markers:

568 vanillylmandelic acid, homovanillic acid and 5-hydroxyindoleacetic acid. Clin Chim
569 Acta. 2008;398(1-2):53-56.

570 [34] Brunner HG, Nelen MR, van Zandvoort P, Abeling NGGM, van Gennip AH,
571 Wolters EC, Kuiper MA, Ropers HH, van Oost BA. X-linked borderline mental
572 retardation with prominent behavioral disturbance: phenotype, genetic localization, and
573 evidence for disturbed monoamine metabolism. Am. J. Hum. Genet. 1993; 52: 1032-
574 1039.

575 [35] Palmer EE, Leffler M, Rogers C, Shaw M, Carroll R, Earl J, Cheung NW, Champion
576 B, Hu H, Haas SA, Kalscheuer VM, Gecz J, Field M. New insights into Brunner
577 syndrome and potential for targeted therapy. Clin. Genet. 2015; doi:10.1111/cge.12589.

578 [36] Codina-Solà M, Rodríguez-Santiago B, Homs A, Santoyo J, Rigau M, Aznar-Laín
579 G, Del Campo M, Gener B, Gabau E, Botella MP, Gutiérrez-Arumí A, Antiñolo G, Pérez-
580 Jurado LA, Cuscó I. Integrated analysis of whole-exome sequencing and transcriptome
581 profiling in males with autism spectrum disorders. Mol Autism. 2015. doi:
582 10.1186/s13229-015-0017-0.

583 [37] Biskup CS, Sánchez CL, Arrant A, Van Swearingen AE, Kuhn C, Zepf FD. Effects
584 of acute tryptophan depletion on brain serotonin function and concentrations of dopamine
585 and norepinephrine in C57BL/6J and BALB/cJ mice. PLoS One. 2012;7(5):e35916.

586 [38] Deventer K, Pozo OJ, Verstraete AG, Van Eenoo P. Dilute-and-shoot-liquid
587 chromatography-mass spectrometry for urine analysis in doping control and analytical
588 toxicology. TrAC Trends in Analytical Chemistry 2014; 55: 1-13.

589 [39] Goldstein DS, Eisenhofer G, Kopin IJ. Sources and significance of plasma levels of
590 catechols and their metabolites in humans. J Pharmacol Exp Ther. 2003;305(3):800-811.

591 [40] Rose DP, Braidman IP. Excretion of tryptophan metabolites as affected by
592 pregnancy, contraceptive steroids, and steroid hormones. Am J Clin Nutr. 1971;24:673-
593 683.

594 [41] Fukuwatari T, Murakami M, Ohta M, et al. Changes in the urinary excretion of the
595 metabolites of the tryptophan-niacin pathway during pregnancy in Japanese women and
596 rats. J Nutr Sci Vitaminol .2004;50:392-398.

597 [42] Bortolato M, Shih JC. Behavioral outcomes of monoamine oxidase deficiency:
598 preclinical and clinical evidence. Int Rev Neurobiol. 2011; 100:13-42.

599 [43] Gracia-Rubio I, Moscoso-Castro M, Pozo OJ, Marcos J, Nadal R, Valverde O.
600 Maternal separation induces neuroinflammation and long-lasting emotional alterations in
601 mice. *Prog Neuropsychopharmacol Biol Psychiatry*. 2015; 65:104-117.

602 [44] Mayo Clinic. [http:// www.mayomedicallaboratories.com](http://www.mayomedicallaboratories.com)

603 [45] Quest Diagnostics. [http:// www.questdiagnostics.com](http://www.questdiagnostics.com)

604 [46] Venta R. Year-long validation study and reference values for urinary amino acids
605 using a reversed-phase HPLC method. *Clin Chem*. 2001;47(3):575-583.

606 [47] Nichkova MI, Huisman H, Wynveen PM, Marc DT, Olson KL, Kellermann GH.
607 Evaluation of a novel ELISA for serotonin: urinary serotonin as a potential biomarker for
608 depression. *Anal Bioanal Chem*. 2012; 402(4):1593-1600.

609 [48] de Jong WH, Wilkens MH, de Vries EG, Kema IP. Automated mass spectrometric
610 analysis of urinary and plasma serotonin. *Anal Bioanal Chem*. 2010;396(7):2609-2616.

611 [49] Zhao J, Chen H, Ni P, Xu B, Luo X, Zhan Y, Gao P, Zhu D. Simultaneous
612 determination of urinary tryptophan, tryptophan-related metabolites and creatinine by
613 high performance liquid chromatography with ultraviolet and fluorimetric detection.
614 *Journal of Chromatography B*, 879 (2011) 2720–2725.

615 [50] Whiting M, Pillai D, McWhinney B, Woollard G, Hoad K, Ellis A, Andersen T,
616 Koetsier S. Reference Ranges for Biogenic Amines and their Metabolites in Urine
617 Observations from a Laboratory Survey. Members of the AACB Biogenic Amines
618 Working Party 2013.

619 [51] Kema IP, Schellings AM, Meiborg G, Hoppenbrouwers CJ, Muskiet FA. Influence
620 of a serotonin- and dopamine-rich diet on platelet serotonin content and urinary excretion
621 of biogenic amines and their metabolites. *Clin Chem*. 1992;38(9):1730-1736.

622 [52] Hiratsuka C, Fukuwatari T, Shibata K. Fate of dietary tryptophan in young Japanese
623 women. *Int J Tryptophan Res*. 2012;5:33-47.

624 [53] Kema IP, de Vries EG, Muskiet FA. Clinical chemistry of serotonin and metabolites.
625 *J. Chromatogr. B* 2000; 747: 33–48.

626 [54] Shibata K, Onodera M. High-performance liquid chromatographic determination of
627 3-hydroxykynurenine with fluorimetric detection; comparison of preovulatory phase and
628 postovulatory phase urinary excretion. *J Chromatogr*. 1991; 570(1):13-18.

FIGURE CAPTIONS

Figure 1. Structures of studied analytes involved in the tryptophan and tyrosine pathways.

LNAA: Large neutral aminoacids, NTs: Neurotransmitters, Val: valine, Leu: leucine, Ile: isoleucine, Met: methionine, Trp: tryptophan, Phe: phenylalanine, Tyr: tyrosine, KYN: kynurenine, 3OH-KYN: 3-hydroxykynurenine, KA: kynurenine acid, AA: anthranilic acid, 3OH-AA: 3-hydroxyanthranilic acid, XA: xanthurenic acid, 5HT: serotonin, DA: dopamine, 5HIAA: 5-hydroxyindoleacetic acid, 3Me-Ty: 3-methoxytyramine, HVA: homovanillic acid.

Figure 2. LC-MS/MS chromatograms obtained for (a) 5HT and 5HT-d₄ both after 2 fold dilution of the urine, (b) 5HT and 5HT-d₄ both after 10 fold dilution of the urine and (c) Leu and Ile using the most sensitive transition (132 → 86) and the most specific ones (132 → 69 for Ile and 132 → 43 for Leu).

Figure 3. LC-MS/MS chromatograms for a urine sample containing 681 ng/mL of Val, 634 ng/mL of Leu, 843 ng/mL of Ile, 1517 ng/mL of Met, 11447 ng/mL of Trp, 451 ng/mL of 5HT, 14582 ng/mL of 5HIAA, 982 ng/mL of Kyn, 5361 ng/mL of KA, 85 ng/mL of 3OH-Kyn, 604 ng/mL of XA, 10 ng/mL of AA, 346 ng/mL of 3OH-AA, 4516 ng/mL of Phe, 1062 ng/mL of Tyr, 166 ng/mL of DA, 26 ng/mL of 3Me-Ty and 2180 ng/mL of HVA.

Figure 4. Urinary 5HT/5HIAA and 5HT/Trp ratios from a control group (n=30) and three persons carrying mutations in the *MAOA* gene, the two male probands (1 and 2) and their heterozygous mother (3).

Tables

Table 1. Molecular weight (MW) and SRM conditions for the selected analytes

Compound	MW	Cone voltage (V)	Precursor ion (m/z)	Species	Collision energy (eV)	Product ion (m/z)
Val	117	15	118	[M+H] ⁺	10	72*
					25	55
Leu	131	15	132	[M+H] ⁺	20	43*
					10	86
Ile	131	15	132	[M+H] ⁺	20	69*
					10	86
Met	149	15	150	[M+H] ⁺	10	104*
					20	56
Trp	204	15	205	[M+H] ⁺	10	188*
					20	146
5HT	176	10	177	[M+H] ⁺	5	160*
		25	160	[M+H-NH ₃] ⁺	20	132
5HIAA	191	25	192	[M+H] ⁺	20	146*
					30	91
Kyn	208	15	209	[M+H] ⁺	20	146*
					10	192
3OH-Kyn	224	15	225	[M+H] ⁺	10	208*
					20	162
KA	189	20	190	[M+H] ⁺	20	144*
					10	172
XA	205	20	206	[M+H] ⁺	20	160*
					10	188
AA	119	25	120	[M+H] ⁺	15	92*
					20	65
3OH-AA	153	10	154	[M+H] ⁺	10	136*
		25	136	[M+H-H ₂ O] ⁺	15	108
Phe	165	15	166	[M+H] ⁺	10	120*
					30	103
Tyr	181	15	182	[M+H] ⁺	10	136*
					20	91
DA	153	15	154	[M+H] ⁺	20	91*
		25	137	[M+H-NH ₃] ⁺	20	91
3Me-Ty	167	10	168	[M+H] ⁺	20	91*
		20	151	[M+H-NH ₃] ⁺	20	91
HVA	182	20	183	[M+NH ₄ -NH ₃] ⁺	10	137*
Trp-d ₅	209	15	210	[M+H] ⁺	10	192

5HT-d ₄	180	10	181	[M+H] ⁺	5	164
5HIAA-d ₄	195	25	196	[M+H] ⁺	20	150
Kyn- ¹³ C ₆	214	15	215	[M+H] ⁺	20	152
3OH-Kyn- ¹³ C ₆	230	15	231	[M+H] ⁺	10	214
KA-d ₅	194	20	195	[M+H] ⁺	20	149
Phe-d ₅	170	15	171	[M+H] ⁺	10	125
Tyr-d ₄	185	15	186	[M+H] ⁺	10	140
DA-d ₄	157	15	158	[M+H] ⁺	20	95
3Me-Ty-d ₄	171	10	172	[M+H] ⁺	20	95

* Transition used for quantification

657
658
659
660

661
662

Table 2. Linearity and LOD for the selected analytes in the different matrices

		Human Urine			Human Plasma			Mice PFC		
		Linearity			Linearity			Linearity		
	Internal standard	Range (ng/mL)	r	LOD (ng/mL)	Range (ng/mL)	r	LOD (ng/mL)	Range ^(a) (ng/mL)	r	LOD ^(a) (ng/mL)
Val	Tyr-d ₄	50-5000	0.998	10	1000-30000	0.992	100**	10-1000	0.998	1
Leu	Tyr-d ₄	50-5000	0.993	25	1000-30000	0.994	100**	10-1000	0.999	5
Ile	Tyr-d ₄	250-25000	0.996	25	1000-30000	0.993	100**	10-1000	0.998	5
Met	Tyr-d ₄	50-5000	0.998	50	1000-30000	0.998	100**	10-1000	0.997	5
Trp	Trp-d ₅	250-25000	0.993	25**	1000-30000	0.995	100**	10-1000	0.996	2
5HT	5HT-d ₄	10-500	0.995	10	2-200	0.997	0.5	1-25	0.995	0.5
5HIAA	5HIAA-d ₄	250-25000	0.991	25**	2-200	0.997	1	0.25-25	0.993	0.1
KYN	Kyn- ¹³ C ₆	50-5000	0.996	50	25-3000	0.995	2.5**	1-25*	0.997	0.5*
3OH-KYN	3OH-Kyn- ¹³ C ₆	25-500	0.983	25	2-200	0.982	2	1-25*	0.995	1*
KA	KA-d ₅	1000-100000	0.996	100**	2-200	0.995	1	0.25-25*	0.994	0.1*
XA	Trp-d ₅	50-5000	0.998	25	-	-	-	-	-	-
AA	5HIAA-d ₄	5-500	0.998	5	0.5-50	0.994	0.3	1-25*	0.996	1*
3OH-AA	Trp-d ₅	25-500	0.991	25	-	-	-	-	-	-
Phe	Phe-d ₅	250-25000	0.998	25**	1000-30000	0.991	100**	10-1000	0.999	1
Tyr	Tyr-d ₄	250-25000	0.998	25**	1000-30000	0.999	100**	10-1000	0.998	2
DA	DA-d ₄	10-500	0.993	10	-	-	-	2.5-250	0.997	2
3Me-Ty	3Me-Ty-d ₄	5-500	0.997	2.5	-	-	-	0.25-25*	0.996	0.1*
HVA	5HIAA-d ₄	1000-25000	0.993	1000	-	-	-	-	-	-

663
664
665

“-“ LOD > endogenous levels, * values obtained after preconcentration of the sample, ** LODs arbitrarily set at 1/10 of the lowest calibration point. ^(a) levels referred to mL of mice PFC extract.

Table 3. Accuracy, precision and matrix effect in the different matrices tested.

Analyte	Matrix	Intra-day (n=6)		Inter-day (n=12)		Matrix effect (n=6)	
		Accuracy (%)	RSD (%)	Accuracy (%)	RSD (%)	Recovery (%)	RSD (%)
Val	Urine	103	13	95	11	81	11
	Plasma	88	13	80	15	55	8
	PFC	97	4	104	13	51	8
Leu	Urine	95	4	91	7	85	4
	Plasma	92	10	93	11	73	3
	PFC	104	3	110	11	102	4
Ile	Urine	108	2	99	9	100	3
	Plasma	98	12	99	12	77	3
	PFC	111	4	116	7	110	5
Met	Urine	114	6	120	11	131	10
	Plasma	89	6	90	12	72	4
	PFC	117	22	105	35	68	30
Trp	Urine	85	10	82	13	101	7
	Plasma	93	13	86	13	87	4
	PFC	89	3	94	10	80	6
5-HT	Urine	101	6	98	10	87	14
	Plasma	105	6	96	12	59	11
	PFC	91	11	95	24	52	35
5HIAA	Urine	96	5	94	5	96	8
	Plasma	94	5	96	6	94	8
	PFC	83	6	87	17	61	18
Kyn	Urine	100	5	100	6	108	7
	Plasma	107	7	107	7	107	2
	PFC	113	9	116	14	290	11
3OH-Kyn	Urine	94	18	102	18	124	16
	Plasma	104	11	110	11	87	15
	PFC	102	11	98	10	192	12
KA	Urine	96	3	98	4	105	5
	Plasma	106	2	93	17	117	4
	PFC	114	4	108	6	173	6
XA	Urine	102	9	107	12	113	14
	Plasma	-	-	-	-	-	-
	PFC	-	-	-	-	-	-
AA	Urine	100	3	96	7	99	3
	Plasma	92	19	107	21	110	15
	PFC	91	6	86	9	128	8
3OH-AA	Urine	92	10	89	12	84	10
	Plasma	-	-	-	-	-	-
	PFC	-	-	-	-	-	-
Phe	Urine	100	6	106	12	113	12
	Plasma	89	9	92	12	75	6
	PFC	93	4	100	11	91	5
Tyr	Urine	99	5	94	7	91	6
	Plasma	89	11	89	12	72	5
	PFC	86	3	101	23	128	6
DA	Urine	92	10	88	12	55	22
	Plasma	-	-	-	-	-	-
	PFC	99	2	111	12	53	6
3Me-Ty	Urine	103	2	105	3	108	5
	Plasma	-	-	-	-	-	-
	PFC	100	8	101	6	64	17
HVA	Urine	100	8	96	8	97	8
	Plasma	-	-	-	-	-	-
	PFC	-	-	-	-	-	-

“-“ LOD > endogenous levels

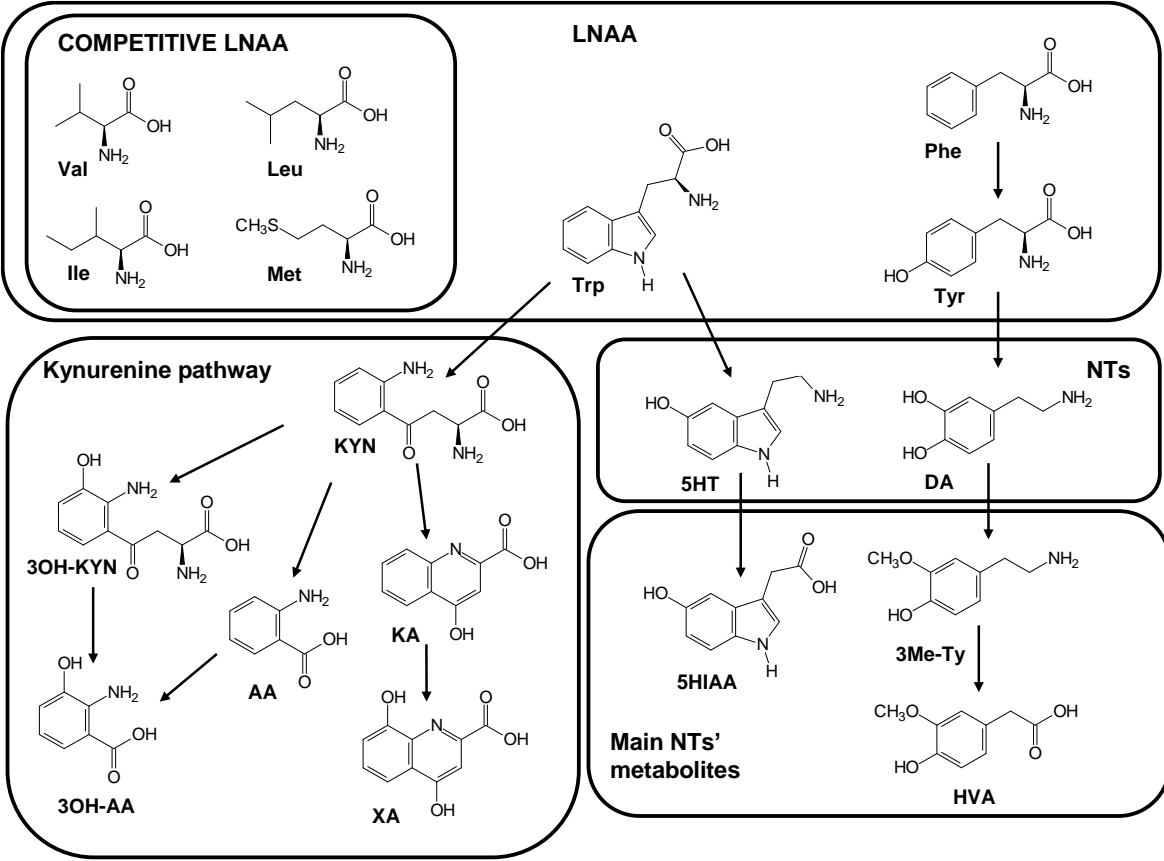
668 **Table 4.** Normal ranges obtained in this study in human adult urine compared with those previously reported.

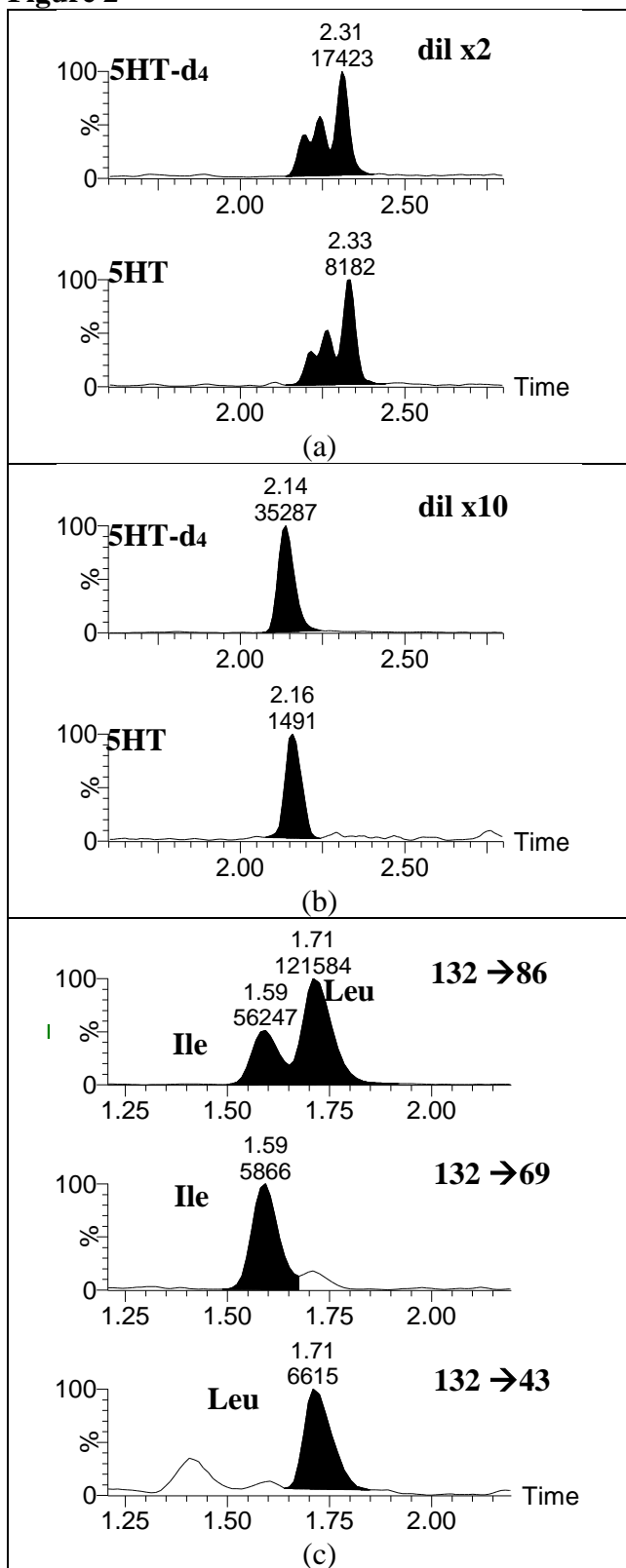
Analyte	ng/mg creatinine			µg/24h					
	Present study	From references		Present study	From references		Present study	From references	
	Range	Range	Ref.	Range	Range	Ref.	Average ± SD	Average ± SD	Ref.
Val	1262-3974	1287-12424	[44-46]	1541-3771	-	-	2476±738	-	-
Leu	2986-11858	2318-18548	[44-46]	3204-18773	-	-	8003±4224	-	-
Ile	1460-4154	1158-10433	[44-46]	797-7367	-	-	3296±1633	-	-
Met	147-1797	1318-6592	[44-46]	148-1584	-	-	713±457	-	-
Trp	7483-24858	3060-25274	[44-46]	8755-37307	-	-	16506±8031	8874±2264	[52]
5-HT	44-211	15-366	[47,48]	47-219	60-167	[53]	132±48	733±341	[52]
5-HIAA	2219-7649	169-5696	[48,49]	2627-14399	382-9550	[53]	5388±3081	3800±1031	[52]
Kyn	266-1316	202-1988	[49]	321-1249	-	-	647±274	786±372	[52]
3OH-Kyn	23-433	-	-	17-678	0.4-7.4	[54]	249±177	828±380	[52]
KA	2017-6053	551-1923	[49]	3133-5744	-	-	4213±834	1884±489	[52]
XA	481-1634	-	-	574-2118	-	-	1051±426	565±315	[52]
AA	3-56	-	-	3-59	-	-	25±17	143±65	[52]
3OH-AA	10-2957	-	-	14-2617	-	-	898±793	820±529	[52]
Phe	3326-13326	2145-18982	[44-46]	4949-15992	-	-	8086±3085	-	-
Tyr	3639-23290	2715-57663	[44-46]	4716-43842	-	-	15698±9931	-	-
DA	48-434	n.d.-812	[50]	35-520	65-400	[44]	248±143	-	-
3Me-Ty	19-80	-	-	26-95	227(mean)		55±23	-	-
HVA	2461-7146	n.d.-16106	[50,41]	4000-8119	0-7280	[51]	1250±8329	-	-

669

670

Figure 1





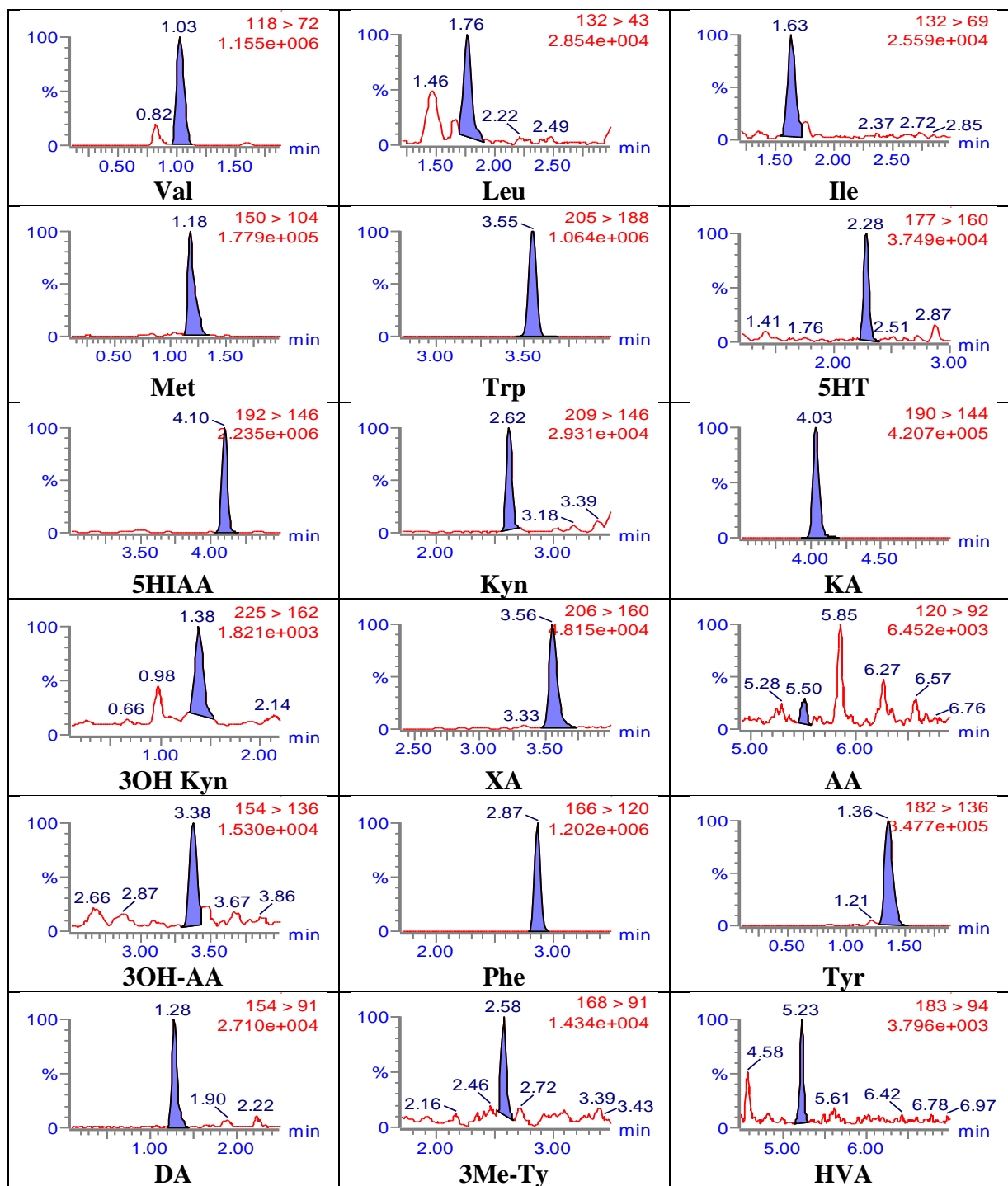


Figure 3

Figure 4.

